Monthly Notices
of the
ROYAL ASTRONOMICAL SOCIETY

MNRAS **468,** 147–153 (2017) doi:10.1093/mnras/stx429

Radial dependence of the dark matter distribution in M33

E. López Fune,[1,2]★ P. Salucci[1,3] and E. Corbelli[4]

[1]*Scuola Internazionale Superiore di Studi Avanzati (SISSA), Via Bonomea 265, 34136 Trieste, Italy*
[2]*Abdus Salam International Centre for Theoretical Physics, Strada Costiera 11, 34151 Trieste, Italy*
[3]*INFN, Sezione di Trieste, Via Valerio 2, 34127, Trieste, Italy*
[4]*INAF–Osservatorio Astrofisico di Arcetri, Largo E. Fermi 5, 50125 Firenze, Italy*

Accepted 2017 February 16. Received 2017 February 10; in original form 2016 November 17

ABSTRACT

The stellar and gaseous mass distributions, as well as the extended rotation curve, in the nearby galaxy M33 are used to derive the radial distribution of dark matter density in the halo and to test cosmological models of galaxy formation and evolution. Two methods are examined to constrain the dark mass density profiles. The first method deals directly with fitting the rotation curve data in the range of galactocentric distances $0.24 \leq r \leq 22.72$ kpc. Using the results of collisionless Λ cold dark matter numerical simulations, we confirm that the Navarro–Frenkel–White (NFW) dark matter profile provides a better fit to the rotation curve data than the cored Burkert profile (BRK) profile. The second method relies on the local equation of centrifugal equilibrium and on the rotation curve slope. In the aforementioned range of distances, we fit the observed velocity profile, using a function that has a rational dependence on the radius, and we derive the slope of the rotation curve. Then, we infer the effective matter densities. In the radial range $9.53 \leq r \leq 22.72$ kpc, the uncertainties induced by the luminous matter (stars and gas) become negligible, because the dark matter density dominates, and we can determine locally the radial distribution of dark matter. With this second method, we tested the NFW and BRK dark matter profiles and we can confirm that both profiles are compatible with the data, even though in this case the cored BRK density profile provides a more reasonable value for the baryonic-to-dark matter ratio.

Key words: galaxies: individual: M33 – galaxies: ISM – galaxies: kinematics and dynamics – dark matter.

1 INTRODUCTION

In the innermost parts of galaxy discs, the luminous matter dominates the dynamics: light traces the mass inferred from disc rotation (Athanassoula, Bosma & Papaioannou 1987; Persic & Salucci 1988; Palunas & Williams 2000) out to a radius ranging between one and three disc exponential scalelengths – depending upon the galaxy luminosity (Salucci & Persic 1999). Instead, in the outskirts, far from galaxy centres, rotational velocities are found to be constant or even rising with radius, despite the sharp radial decrease of the stellar or gaseous surface brightness. This contradicts the well-known Keplerian-like expectations of the standard Newtonian gravity if light traces the mass. It is well known that, in order to explain this anomaly, a dark matter (DM) halo is routinely added in the computation of the gravitational potential (Bosma 1978; Bosma & van der Kruit 1979; Rubin, Thonnard & Ford 1980). The luminous and DM contributions to the rotation curve (RC) can explain the observed velocities as traced by starlight or gas emission, even at large galactocentric distances where rotational velocities are flat or keep increasing with radius.

However, it is well known that collisionless and stable weakly interacting massive particles (WIMPs) in a Λ cold dark matter (ΛCDM) cosmology, provide a major scenario to frame the DM in galaxies and in the Universe. Cosmological simulations show that the DM density distribution $\rho_{\rm DM}$ is nearly universal (i.e. dependent only on the mass of the halo). This density profile has a characteristic steep slope (cusp) in the inner regions, which can be approximated by a power law $\rho(r)/\rho_{\rm c} \simeq (r/r_{\rm c})^{-\gamma}$, where $\rho_{\rm c}$ is a characteristic constant density, γ is of order unity and $r_{\rm c}$ is a constant scaling radius.

This cuspy density profile has not been inferred for several dwarfs, spirals and low-surface-brightness galaxies (Moore 1994; Salucci & Burkert 2000; de Blok & Bosma. 2002; de Blok et al. 2008; Gentile et al. 2004, 2005; Oh et al. 2015) whose RCs favour a much shallower cored profile. In addition, independent evidence for a cored distribution comes from stacked RCs, which lead to an almost solid body profile $V \propto r$ at $r \to 0$ (Salucci et al. 2007; Donato et al. 2009; Karukes & Salucci 2017). All this evidence, though remarkable, still needs some investigation because the

★ E-mail: elopez@sissa.it

inner regions of galaxies are dominated by the luminous matter. The cusp–core issue in galaxy DM density profiles is also related to the investigation of the nature of the DM itself and to the galaxy evolution. Numerical simulations have, in fact, shown that baryonic feedback occurring at later times than the galaxy formation epoch can transform the original NFW profiles into cored profiles (Di Cintio et al. 2014; Chan et al. 2015). Hence, the existence of cores for DM halo density distributions in dwarf galaxies might not be sufficient to disprove the ΛCDM scenario. Specifically, for the same galaxy we need very accurate mass models and a high-quality RC that traces, with high resolution, the inner disc kinematics (using mm or optical line tracers) and extends radially for several disc scalelengths (because of the outer disc 21-cm line emission of neutral hydrogen).

In this paper, we study in detail the DM distribution in M33, a Local Group low-luminosity spiral galaxy, rich in gas and very much DM-dominated. Its RC is very extended because of the presence of a large gaseous disc and it has an excellent spatial resolution because of the proximity of M33 and the presence of CO lines that trace the inner kinematics (Corbelli 2003; Corbelli et al. 2014). The high-resolution RC of this galaxy makes it possible for us to derive the DM halo distribution from the inner regions out to large galactocentric distances and therefore to uniquely test the ΛCDM cosmological scenario. M33 does not host a bulge or a prominent bar (Corbelli & Walterbos 2007): the absence of these concentrated stellar distributions much alleviates the usual uncertainty in deconvolving the disc contribution from that of a bulge, and in modelling correctly non-circular motion. It is important to stress the crucial result obtained for this object by Corbelli et al. (2014). They have inferred the stellar mass surface density locally by measuring the pixel spectral energy distribution(SED) and fitting population synthesis models pixel-by-pixel. This method provides a map of the stellar mass density and a good estimate of its radial profile, which previously has been assumed to be proportional to the luminosity profile. This reduces considerably the uncertainties on the contribution of luminous matter to the galaxy circular velocity (Corbelli et al. 2014). The gaseous disc mass contribution can be obtained directly from the H I surface photometry given the well-known distance of the galaxy.

In Corbelli et al. (2014), the DM density has been derived using detailed maps of the stellar surface density in connection with a standard fit (via χ^2 minimization) of the observed RC. The mass model considered by the authors includes a stellar plus a gaseous disc, and a DM halo. The latter is assumed to have a Navarro–Frenkel–White (NFW) or, alternatively, a cored Burkert (BRK) radial density profile, both with two free parameters to be determined by the RC fit. Their results indicate that both models give a satisfactory RC fit, even though the NFW profile provides a better fit. The DM halo density profile cannot be uniquely determined because the luminous matter significantly contributes to the total gravitational potential in the inner parts of the galaxy. Only for spirals or dwarfs with maximum velocities <70 km s^{-1} does the RC directly measure the DM profile in the inner regions. In objects such as M33, instead, even the small uncertainties left in modelling the stellar disc mass propagate into the inferred DM halo density, leaving some uncertainties on its mass and radial density profile.

To better constrain the DM density distribution, it is possible to use a second scheme in which the RC and dynamical mass modelling are analysed only in regions that are not much affected by the luminous matter distribution (Salucci et al. 2010). This method, discussed in Salucci et al. (2010), has been applied first to the Milky Way and then to the spiral galaxy NGC 3198 (Karukes, Salucci & Gentile 2015). It allows us to derive very precisely the DM density in the outskirts of a galaxy, provided that the H I surface density is well known and that the circular velocity and its first derivative are accurately determined, so that $\delta V/V < 0.05$, $\delta \mathrm{d}\log V/\mathrm{d}\log r < 0.1$. Using this method, in this paper we investigate whether the RC of M33 is compatible with the ΛCDM halo density profile or with a cored halo density profile. We have adopted the BRK halo profile to represent the latter, following Salucci et al. (2007) and Karukes & Salucci (2017) who have analysed the DM halo contribution to the universal RC of spirals.

The paper is organized into four sections. In Section 2, we summarize the observed RC of M33, the three main baryonic components of M33's disc, their corresponding surface mass densities and their contributions to the RC. We also outline the results of the previous dynamical analysis (Corbelli et al. 2014). In Section 3, we develop a local modelling technique that does not rely on any of the global mass modelling of the galaxy and we obtain a very robust and careful determination of the DM halo density of M33. Finally, in Section 4, we summarize the main conclusions of this work.

2 LUMINOUS AND DARK MATTER CONTRIBUTIONS TO THE ROTATION CURVE

In this section we introduce the stellar and gaseous components of M33's disc and we discuss the radial dependence of the baryonic surface mass density as derived by Corbelli et al. (2014). We then briefly summarize how these baryonic mass distributions are used for the standard RC fitting method in M33 and we discuss the implications for the DM distribution.

2.1 Stellar and gaseous discs

Because of the tight correlations between the colour and the apparent stellar mass-to-light ratio M/L (Bell & de Jong 2001), the stellar mass, to a first approximation, can be determined using multiband optical imaging measurements of the whole galaxy luminosity in several bands. However, there are likely radial variations of the stellar mass-to-light ratio, as galaxy discs grow with time. Portinari & Salucci (2010), Zibetti, Charlot & Rix (2009) and González Delgado et al. (2014) have been using chemo-photometric models for large samples of spatially resolved, disc-dominated galaxies to determine the radial dependence of the stellar mass surface density. A radially decreasing mass-to-light ratio is found based on galaxy colour gradients and spectral synthesis techniques. As M33 is the second closest spiral, Corbelli et al. (2014) implemented an extension of the ZCR09 method to build up a detailed map of the stellar surface mass density using mosaic maps in the *B*, *V*, *I*, *g* and *i* bands from the Local Group Survey (Massey et al. 2006) and from the Sloan Digital Sky Survey (SDSS Collaboration 2000). After processing the images, a pixel-by-pixel synthesis model of the stellar population made it possible to obtain a stellar mass surface density map of the M33 disc out to 5 kpc, which showed a clear radial gradient of the mass-to-light ratio in the inner regions. This finding is consistent with the negative radial metallicity gradient, which supports an inside-out formation scenario and underlines the importance of carrying out a careful analysis of the stellar mass distribution in discs before computing their contribution to RCs (Portinari & Salucci 2010). By fitting the resulting radial averages of the stellar surface mass density of M33, with analytical functions (i.e. exponential functions with different scalelengths r_s), Corbelli

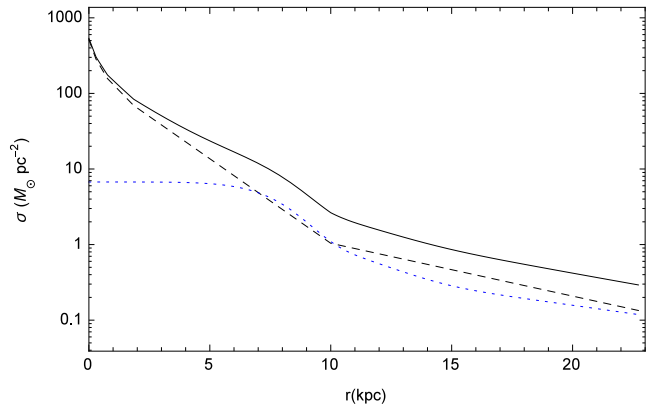

Figure 1. Radial dependence of the baryonic mass surface densities of the disc of M33: stellar surface density inferred from *BVIgi* maps (dashed line), the neutral hydrogen surface density (dotted line) and the total baryonic mass surface density (solid line) – namely stars and atomic and molecular gas.

et al. (2014) obtained the following approximation for the radial distribution of the stellar mass surface density in units of $M_\odot$ pc^{-2}:

$$\sigma_{BVIgi}(r) = \begin{cases} \exp(-2.010\,r + 6.24), & 0.0 < r \leq 0.3\,\mathrm{kpc} \\ \exp(-1.239\,r + 6.01), & 0.3 < r \leq 0.77\,\mathrm{kpc} \\ \exp(-0.758\,r + 5.64), & 0.77 < r \leq 1.85\,\mathrm{kpc} \\ \exp(-0.515\,r + 5.19), & 1.85 < r \leq 10\,\mathrm{kpc} \\ \exp(-0.161\,r + 1.65), & 10 < r \leq 23\,\mathrm{kpc} \end{cases} . \quad (1)$$

Here, r is the galactocentric radius in kpc units. The fits to the radial distribution of the stellar mass density are shown in Fig. 1 (dashed line), where we can see that the stellar mass density drops by more than three orders of magnitudes from the centre to the outskirts of M33's disc. The amplitude of $\sigma_{BVIgi}(r)$ is uncertain by 30 per cent, while its radial trend has negligible uncertainties. As in Corbelli et al. (2014), in order to compute the dynamical contribution of the stellar mass density to the RC, we consider the stellar disc perpendicular to the galactic plane as a flaring disc with a radially varying half thickness; this is only 100 pc at the centre and it reaches 1 kpc at the edge of the outer disc.

The gaseous disc is made of atomic and molecular gas (mostly hydrogen and helium) and it warps beyond 8 kpc. The high-resolution 21-cm data for the atomic hydrogen gas in M33, the best-fitting tilted ring model and the radial averages of the H I surface density distribution, $\sigma_{\rm HI}(r)$, have been presented by Corbelli et al. (2014). In the same paper, the authors summarize the results of the CO surveys for the determination of the H_2 surface mass density. The molecular gas surface density is well represented by the following relation: $\Sigma_{H_2} = 10 \exp(-r/2.2)$ M$_\odot$ pc^{-2} where r is in kpc (Corbelli 2003; Gratier et al. 2010; Druard et al. 2014). For the dynamical contribution of the gaseous disc to the RC, the gaseous disc has been considered vertically thick with a half thickness of 0.5 kpc.

Using the accurate determination of the stellar mass surface density via chemo-photometric methods, we can determine the total baryonic matter surface density in M33 shown in Fig. 1. In the inner regions of the galaxy ($r \lesssim 7$ kpc; see Fig. 1), the stellar mass surface density dominates over the gaseous mass surface density. For $7 \lesssim r \lesssim 10$ kpc, stars and atomic gas have a similar mass surface density and beyond 10 kpc, they decrease with radius with a similar slope.

In the standard RC fitting method used by Corbelli et al. (2014), the stellar and gaseous disc velocity contributions add in quadrature as follows:

$$V_{\rm d}^2(r) = \Upsilon V_{\rm s}^2(r) + V_{\rm g}^2(r). \quad (2)$$

Here, $\Upsilon = \Upsilon_*/\Upsilon_*^{BVIgi} = M_*/M_*^{BVIgi}$ is the ratio between the stellar disc mass and that given by equation (1), which is 4.9×10^9 M$_\odot$ out to $r = 23$ kpc. The parameter Υ takes into account the uncertainties in the stellar disc mass, and hence the total stellar disc mass is allowed to vary in the interval 3.4–6.4 $\times$ 10^9 M$_\odot$. The terms $V_{\rm s}(r)$ and $V_{\rm g}(r)$ indicate the contributions to the RC of the stellar disc, as given by equation (1), and of the helium-corrected H I and H_2 gas mass.

2.2 Dark matter halo models and dynamical analysis of the rotation curve

The standard dynamical analysis of the RC is carried out by modelling the galaxy with a DM halo and stellar and gaseous disc mass surface densities in the whole sampled radial range ($0.24 \leq r \leq 23$ kpc for M33). Two different DM halo models have been considered by Corbelli et al. (2014) in fitting the M33 RC. The first is a halo with a NFW density profile for structures growing in a ΛCDM hierarchical universe (Navarro, Frenk & White 1996, 1997; Klypin et al. 2001; Caimmi & Marmo 2004; Hayashi et al. 2004; Diemand et al. 2005), given by

$$\rho_{\rm NFW}(r) = \frac{\rho_{\rm c}}{(r/r_{\rm c})[1 + (r/r_{\rm c})]^2}, \quad (3)$$

where $\rho_{\rm c}$ and $r_{\rm c}$ are the two usual halo parameters. The contribution of the DM density profile adds in quadrature to the disc contribution to give the total rotational velocity as

$$V^2(r) = V_{\rm NFW}^2(r) + V_{\rm d}^2(r), \quad (4)$$

$$V_{\rm NFW}^2(r) = \frac{4\pi G \rho_{\rm c} r_{\rm c}^2}{r/r_{\rm c}} \left\{ \ln[1 + (r/r_{\rm c})] - \frac{r/r_{\rm c}}{1 + (r/r_{\rm c})} \right\}. \quad (5)$$

The virial mass $M_{\rm vir}$ and the concentration parameter $c = r_{\rm vir}/r_{\rm c}$, are related to $\rho_{\rm c}$ and $r_{\rm c}$ by

$$\rho_{\rm c} = \frac{97.2}{3} \frac{c^3}{\ln(c+1) - [c/(c+1)]} \rho_{\rm crit} \ \ \mathrm{gcm}^{-3}, \quad (6)$$

$$r_{\rm c} = \frac{1}{c} \left(\frac{3}{97.2} \frac{M_{\rm vir}}{4\pi\rho_{\rm crit}} \right)^{1/3} \ \ \mathrm{kpc}. \quad (7)$$

where $r_{\rm vir}$ is the virial radius and $\rho_{\rm crit} = 9.3 \times 10^{-30}$ g cm^{-3} is the critical density of the Universe. The free parameters c and $M_{\rm vir}$ were determined as independent parameters but, after the RC fit, the authors checked the consistency of their values with the relations obtained by numerical simulations of structure formation in a ΛCDM universe. The free parameters of this halo model, $M_{\rm vir}$ and c, are in fact not independent of each other (Bullock et al. 2001). Recent numerical simulations (Dutton & Macciò 2014) suggest a correlation, which can be expressed using the dimensionless value of the Hubble parameter $h = 0.678$ (Planck Collaboration XIII 2016) as

$$c = 10.6 \left(\frac{1}{10^{12} h^{-1}} \frac{M_{\rm vir}}{M_\odot} \right)^{-0.097}. \quad (8)$$

The values $c = (9.5 \pm 1.5)$, $M_{\rm vir} = (4.3 \pm 1.0) \times 10^{11}$ M$_\odot$ and $M_* = (4.9 \pm 0.6) \times 10^9$ M$_\odot$ have been obtained by Corbelli et al. (2014) by considering a composite probability, which takes

into account the fit to the RC, the synthesis models of the stellar population and the c–$M_{\rm vir}$ relation found by numerical simulations.

The second halo profile considered by Corbelli et al. (2014) is the phenomenological cored BRK density distribution, which successfully fits individual RCs (see Gentile et al. 2005, and references therein), as well as the universal rotation curve of spirals. This cored halo profile, also known as the Burkert halo profile (Burkert 1995, 1996; Salucci & Burkert 2000), has a radial density distribution given by

$$\rho_{\rm BRK}(r) = \frac{\rho_{\rm c}}{[1+(r/r_{\rm c})][1+(r^2/r_{\rm c}^2)]}, \tag{9}$$

where $\rho_{\rm c}$ and $r_{\rm c}$ are the central density and the core radius, respectively. This density profile induces a gravitational potential such that every particle in the galactic disc rotates with a velocity $V_{\rm BRK}$, which adds in quadrature to the velocity induced by the baryonic disc component as

$$V^2(r) = V^2_{\rm BRK}(r) + V^2_{\rm d}(r) \tag{10}$$

and

$$V^2_{\rm BRK}(r) = \frac{2\pi G\rho_{\rm c} r_{\rm c}^2}{r/r_{\rm c}}\Big\{\ln[1+(r/r_{\rm c})] + \ln\sqrt{1+(r/r_{\rm c})^2} - \tan^{-1}(r/r_{\rm c})\Big\}. \tag{11}$$

The central core density $\rho_{\rm c}$ and the scaling radius $r_{\rm c}$ are not independent either, as shown in Donato et al. (2009), and the following relation holds:

$$\log\left(\frac{\rho_{\rm c} r_{\rm c}}{{\rm M}_\odot\ {\rm pc}^{-2}}\right) = 2.15 \pm 0.2. \tag{12}$$

vv

Through the dynamical analysis of the M33 RC, Corbelli et al. (2014) found no compatible values of the stellar mass surface densities using equation (1). However, considering only the B, V, I colour maps of M33, the synthesis models predict higher stellar masses than equation (1): 5.5×10^9 M$_\odot$. Given the uncertainties in the models, the likely M33 stellar mass is, in this case, within the interval 3.9–7.2 $\times$ 10^9 M$_\odot$. Using the corresponding stellar mass surface density, the following RC best-fitting values for the BRK halo and the stellar mass have been found: $r_{\rm c} = 7.5$ kpc, $\rho_{\rm c} = 18.0 \times 10^6$ M$_\odot$ kpc^{-3} and $M_* = 7.2 \times 10^9$ M$_\odot$. The global χ^2 value is larger than that found when using the NFW DM profile but it is still acceptable. Therefore, even for this galaxy, although we have accurate and extended RC data tracing the gravitational potential, and a good determination of the baryonic mass surface density, both DM mass models are compatible with the data. This can be easily attributed to the fact that in M33, even beyond 10 kpc, the influence of the luminous matter is not negligible, so any derivation of the DM density profile would be fraught with the uncertainties inherent to such a component. More precisely, because in the inner regions $r \lesssim 2R_{\rm D}$ (where $R_{\rm D}$ is the disc lengthscale) of most spirals, the stellar disc dominates over the dark component, and even small uncertainties in the mass determination of the former induce large uncertainties in the values of the structural parameters of the dark components. By using a second method for fitting the RC data in the next section, we hope to alleviate this degeneracy. We will see that the fit related to the second method is less dependent on the luminous matter distribution and thus hopefully it will help us to clarify better the properties of the DM halo that hosts M33.

3 MODEL-INDEPENDENT METHOD FOR LOCAL DENSITY ESTIMATION

A new method to determine the DM density distribution in spiral galaxies has been introduced by Salucci et al. (2010). This method was applied first to estimate the value of the DM density at the Sun's location (Salucci et al. 2010), and extended in Karukes et al. (2015) to the study of the DM distribution in the galaxy NGC 3198. The goal of this section is to derive, for the spiral galaxy M33, a model-independent DM density using this method, which deals with the RC at large radii, where the influences of the stellar and gaseous discs are weak.

3.1 Local density estimation method

The idea, introduced by Salucci et al. (2010), is to resort to the equation of centrifugal equilibrium, which holds the spiral galaxies:

$$\frac{V^2}{r} = a_{\rm h} + a_{\rm s} + a_{\rm g}. \tag{13}$$

Here, $a_{\rm h}$, $a_{\rm s}$ and $a_{\rm g}$ are the radial accelerations, generated by the DM halo and stellar and gaseous discs, respectively.

Under the approximation of a spherical DM halo, we have

$$\rho_{\rm h}(r) = \rho(r) - \Upsilon\rho_{\rm s}(r) - \rho_{\rm g}(r) = \frac{X_q}{4\pi G r^2}\frac{\rm d}{{\rm d}r}\left(rV^2 - r\Upsilon V_{\rm s}^2 - rV_{\rm g}^2\right), \tag{14}$$

$$\rho(r) = \frac{1}{4\pi G r^2}\frac{\rm d}{{\rm d}r}\left(rV^2\right), \tag{15}$$

$$\rho_{\rm s}(r) = \frac{1}{4\pi G r^2}\frac{\rm d}{{\rm d}r}\left(rV_{\rm s}^2\right) \tag{16}$$

and

$$\rho_{\rm g}(r) = \frac{1}{4\pi G r^2}\frac{\rm d}{{\rm d}r}\left(rV_{\rm g}^2\right). \tag{17}$$

Here, X_q is a factor correcting the spherical Gaussian law used above in the case of an oblate DM halo and it takes values between 1.05 and 1.00 (see details in Salucci et al. 2010), $V(r)$ is the velocity given by the RC, $V_{\rm s}$ and $V_{\rm g}$ are the stellar and gas velocities, respectively, and Υ, as usual, is the stellar mass-to-light ratio. The strength of this method lies in the fact that we have transformed the surface mass density of the stellar and gaseous discs in equivalent bulk densities with the aid of the Gaussian law. Because the velocities induced by the stellar and gaseous discs decrease slowly after 9.53 kpc, we expect a sharp fall for their equivalent three-dimensional densities $\rho_{\rm s}$ and $\rho_{\rm g}$, and we are left with only the DM contribution to the observed RC. From this fact, we can infer the DM halo properties directly from the experimental data.

An issue left to treat is to derive an analytical expression for the total velocity $V(r)$ from the available discreet set of the RC data. Having an analytical function will avoid artefacts due to the numerical computation of the derivative of $V(r)$ needed for the computation of the total density, as given by equation (15). The following subsection is devoted to finding an appropriate empirical smooth curve to solve this problem.

3.2 Empirical velocity profile

With the aid of the local density method, we can study, directly from the experimental data, the DM halo properties by computing the densities given by equations (15), (16) and (17), respectively. For the purpose of deriving a smooth profile of ${\rm d}V/{\rm d}r$, we introduce

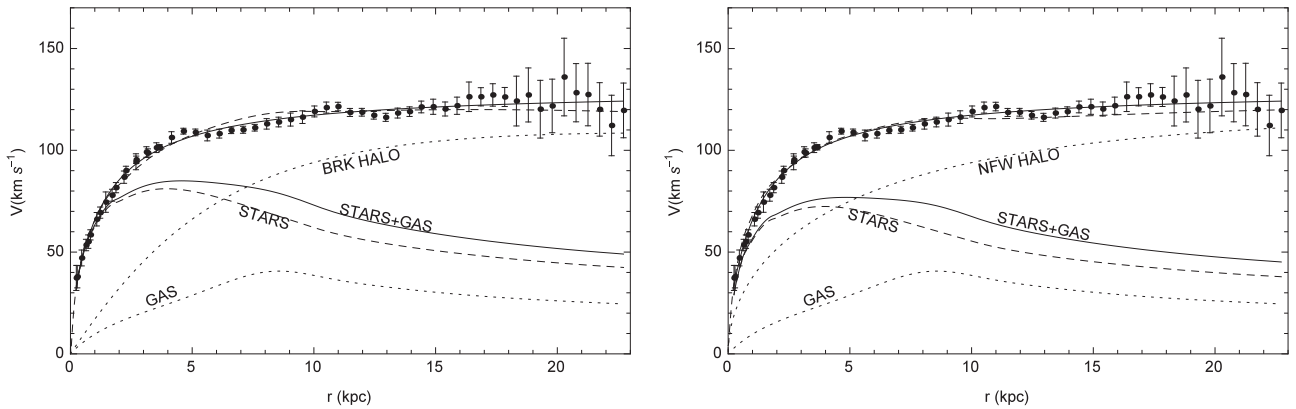

Figure 2. RC of M33 (black dots with error bars) with the analytical best fit to it as given by equation (18) (solid line) with $V_0 = 130.2$ km s^{-1}, $r_0 = 1.3$ kpc and $d = 0.12$. In both panels, we also show (dashed lines with no labels), for comparison, the solutions to the RC fit obtained by Corbelli et al. (2014) using equations (10) and (4) (left and right panels, respectively), as discussed in Section 2. The halo, stellar, gas and total disc contributions are also shown with their corresponding labels.

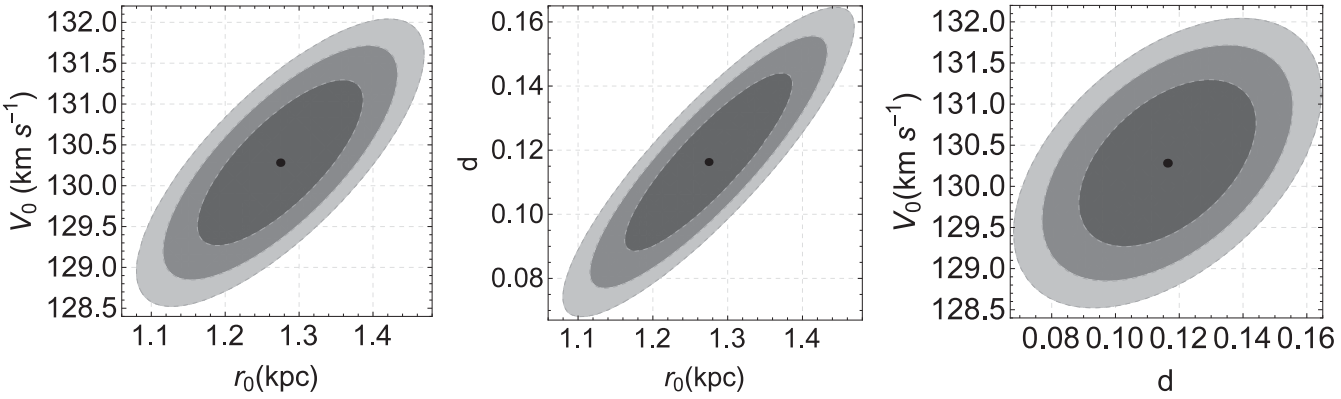

Figure 3. 1σ, 2σ and 3σ confidence ellipses (from dark to light) for the best-fitting parameters V_0, r_0 and d in fitting the analytical function in equation (18) to RC data. The black central dots indicate the best-fitting values.

the following an empirical velocity formula to describe the RC of M33:

$$V(r) = V_0 \frac{(r/r_0) + d}{(r/r_0) + 1}. \quad (18)$$

This is a simple, rational, three-parameter-dependent velocity profile that reproduces, at large galactocentric distances, a flat velocity curve. As we will see immediately, it describes genuinely the RC in the range allowed by the experimental data. The three free parameters – i.e. the terminal velocity V_0, the scaling radius r_0 and $d < 1$, which is an additional parameter to prevent $V(r)$ from being constant – make the degree of freedom of the fit similar to that of the standard RC fitting method (see Section 2) when considering the uncertainties on the stellar surface mass density. The empirical velocity formula can be used when considering both the BRK halo plus luminous disc and the NFW halo plus luminous disc mass models.

By minimizing the χ^2 distribution for fitting the RC data with its measurement errors, with the above analytical function, we obtain the best-fitting parameters: $V_0 = (130.2 \pm 1.0)$ km s^{-1}, $r_0 = (1.3 \pm 0.1)$ kpc and $d = (0.12 \pm 0.03)$, giving $\chi^2_{\rm red} = 0.75$. In Fig. 2, we show the fit to the RC data of the derived analytical function. For comparison, we also show the fits obtained by Corbelli et al. (2014) using the BRK DM profile (left panel) and the NFW DM profile (right panel), as discussed in Section 2. Moreover, in Fig. 3, we show the 1σ, 2σ and 3σ confidence levels for three such free parameters.

3.3 Dark matter profiles and effective densities

Given the goodness of the fit of the RC data with the analytical function given by equation (18), the goal of this subsection is to use this continuous smooth curve to compute $\rho(r)$, as given by equation (15), and the effective baryonic disc densities. As mentioned previously, for $r \gtrsim 9$ kpc, the contributions of the star and gas densities are negligible in equation (14) and we are left only with the DM halo contribution.

In the range of galactocentric distances $9.5 \leq r \leq 22.72$ kpc, we fit the derived density profile using the BRK and NFW DM radial density distributions. In the case of the BRK profile, we obtain the best-fitting values: $r_c = (9.6 \pm 0.5)$ kpc and $\rho_c = (12.3 \pm 1.0) \times 10^6$ M$_\odot$ kpc^{-3}, respectively, giving $\chi^2_{\rm red} = 0.8$, and the halo virial mass is $M_{\rm vir}(3.0 \pm 0.8) \times 10^{11}$ M$_\odot$. In the left panel of Fig. 4, we show the corresponding fit in log–log scale. Framed by this solution, let us stress again that close to $r \sim 9$–9.5 kpc, the stars and gas contributions drop sharply more than two orders of magnitude. Therefore, in the radial range $9.53 \leq r \leq 22.72$ kpc, the stellar mass-to-light ratio Υ plays no role in this analysis and we can obtain the two halo parameters also if the baryonic disc mass has some uncertainties. In the right panel of Fig. 4, we show

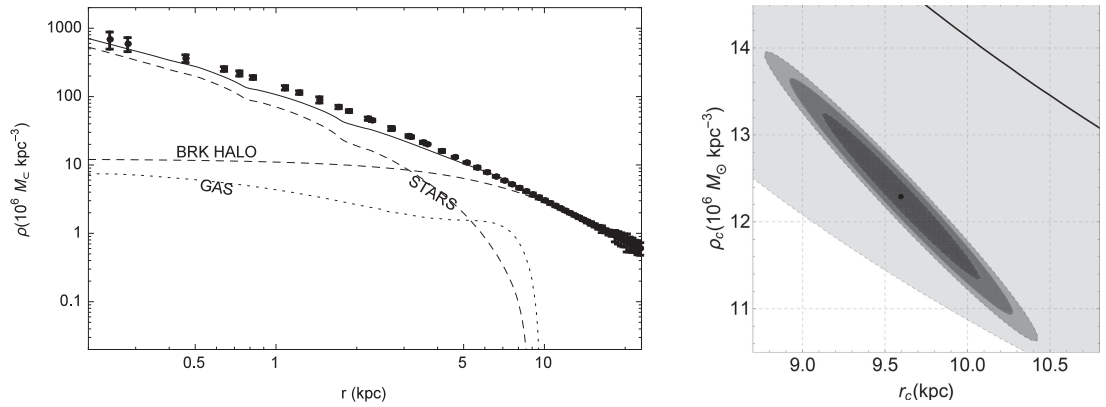

Figure 4. The left panel shows the dependence of various effective densities on galactocentric radius: the black points with error bars correspond to $\rho(r)$ as derived from equation (15), and the solid line marks the total density given by the BRK halo plus stars and gas. We also plot the effective densities of stars and gas given by equations (16) and (17), respectively, and the best-fitting BRK DM halo density. The right panel shows the 1σ, 2σ and 3σ confidence ellipses (from dark to light) for the best-fitting parameters r_c and ρ_c, as well as the correlation between these two (solid line) given by equation (12) with 20 per cent uncertainty (shaded area).

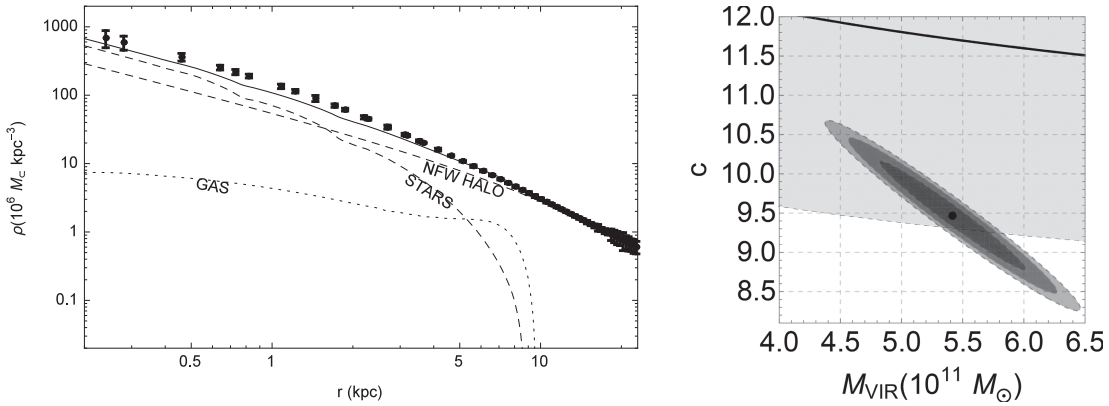

Figure 5. The left panel shows the dependence of various effective densities on galactocentric radius: the black points with error bars correspond to $\rho(r)$ as derived from equation (15), and the solid line marks the total density given by the NFW halo plus stars and gas. We also plot the effective densities of stars and gas given by equations (16) and (17), respectively, and the best-fitting NFW DM halo density. The right panel shows the 1σ, 2σ and 3σ confidence ellipses for the best-fitting halo parameters c and $M_{\rm vir}$, where the black central point corresponds to the best-fitting values of c and $M_{\rm vir}$. The solid line and shaded area in the right panel correspond to the c–$M_{\rm vir}$ correlation given by equation (8).

the corresponding 1σ, 2σ and 3σ confidence levels for the two BRK halo parameters. In the same panel, the solid line shows the correlation found (equation (12)) and the shaded area shows its 1σ region. Clearly, the solution obtained for the parameters ρ_c and r_c lies inside the uncertainties associated with the correlation, as reported in Donato et al. (2009).

We performed the same analysis using the NFW profile. In this case, we obtained the best-fitting values $c = (9.5 \pm 0.7)$ and $M_{\rm vir} = (5.4 \pm 0.6) \times 10^{11}$ M$_\odot$, giving $\chi^2_{\rm red} = 1.0$. In the left panel of Fig. 5, we show the corresponding fit in log–log scale. In the right panel, we display the corresponding 1σ, 2σ and 3σ confidence levels for the two free parameters of the NFW profile, as well as their correlation found by numerical simulations and its uncertainties as given by equation (8) (shaded area).

It is worth discussing the present result. We can trace the distribution of matter in M33 by using the RC observational data, starting from the innermost radius $r = 0.24$ kpc. Inside this radius, no information can be inferred except by extrapolating the best-fitting models and testing the predicted RC velocities with follow-up higher-resolution observations. In the radial range $0.24 \leq r \lesssim 9$ kpc, the stellar component is dynamically very relevant with respect to the DM halo component. For both DM halo models tested, the structural parameters of the DM distribution are mingled with the unknown value of the disc mass. In both cases, no information can be extracted either, as any measurements of DM distribution would be fraught with uncertainties because of the stellar contribution (i.e. the stellar disc accounts for most of the total gravitational potential of the galaxy). Around 9 kpc, the luminous matter still competes against DM to dominate over the total mass, given the RC uncertainties. However, beyond 9.5 kpc, at $\simeq 3.5 R_{\rm D}$, the exponential decrease of the stellar matter density and the negligible contribution of the gaseous component, which never plays a role even if its total mass is about half of that of the stars, ensure that only the DM component balances the radial accelerations that the gaseous disc is engaged with.

In Fig. 6, we show the best fits of the BRK and NFW profiles to the outer disc effective matter densities. As we can see, the values and radial gradients of the matter density of the two DM halo models are similar, in agreement with our finding that both haloes are compatible with the data. This is because the core of the BRK best-fitting halo does not extend much beyond the optical disc, where DM is the dominant dynamical component.

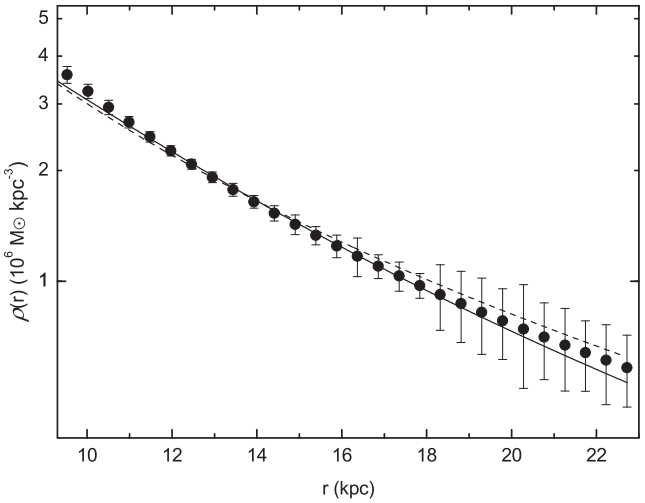

Figure 6. The figure shows the observed DM halo density profile in the outer disc (black dots with error bars). For comparison, we also display the BRK (solid line) and NFW (dashed line) best-fitting halo models to the effective densities inferred from the dynamical analysis of RC data.

4 CONCLUSIONS

In this paper, we have extended the results of Corbelli et al. (2014), who obtained a global fit of the RC of M33, after an accurate mass modelling of its stellar disc, by considering a DM halo with a cuspy NFW or a cored BRK profile. The results of the global fit to the RC favour a cuspy ΛCDM halo despite the fact that a cored halo is still compatible with the data when a heavy stellar disc is considered. Following Salucci et al. (2010) and Karukes et al. (2015), we then use a new approach to investigate the DM content of M33. Relying on the centrifugal equilibrium condition, and assuming a spherical DM halo, we trace the DM density by using only the experimental RC. This method relies on fitting the DM density distribution of M33 in the radial range $9.53 \leq r \leq 22.72$ kpc, where the stellar and gaseous contributions to the RC are negligible. According to this method, the BRK profile with the parameters $r_c = (9.6 \pm 0.5)$ kpc and $\rho_c = (12.3 \pm 1.0) \times 10^6$ $M_\odot$ kpc^{-3} provides an excellent fit to the M33 data. The BRK halo virial mass is $M_{vir} = (3.0 \pm 0.8) \times 10^{11}$ $M_\odot$ and it is only $6.7 \pm 1.2 \times 10^{10}$ $M_\odot$ out to about 23 kpc. When testing the NFW DM profile through the local density estimator method, we find instead a higher virial mass for the halo and, therefore, an extremely low baryonic fraction. With the analysis presented in this paper, we conclude that the possibility that M33 harbours a cored DM halo still seems to be suitable. Even though the determination of the stellar disc mass via synthesis models has eliminated most of the disc–halo degeneracies in this low-luminosity spiral, we have shown that the degeneracy of cuspy or cored DM density profiles still holds because different dynamical methods used in modelling RC data favour different DM density distributions and halo masses.

ACKNOWLEDGEMENTS

The authors would like to thank Ekaterina Karukes for her assistance, comments and suggestions, as well as the referee and editor in chief of MNRAS for comments that greatly improved the manuscript.

REFERENCES

Athanassoula E., Bosma A., Papaioannou S., 1987, A&A, 179, 23
Bell E. F., de Jong R. S., 2001, ApJ, 550, 212
Bosma A., 1978, PhD Thesis, Groningen Univ.
Bosma A., van der Kruit P. C., 1979, A&A, 79, 281
Bullock J. S., Kolatt T. S., Sigad Y., Somerville R. S., Kravtsov A. V., Klypin A. A., Primack J. R., Dekel A., 2001, MNRAS, 321, 559
Burkert A., 1995, ApJ, 447, L25
Burkert A., 1996, in Bender R., Davies R. L., eds, Proc. IAU Symp. 171, New Light on Galaxy Evolution. Kluwer, Dordrecht, p. 175
Caimmi R., Marmo C., 2004, Serb. Astron. J., 169, 11
Chan T. K., Kereš D., Oñorbe J., Hopkins P. F., Muratov A. L., Faucher-Giguère C.-A., Quataert E., 2015, MNRAS, 454, 2981
Corbelli E., 2003, MNRAS, 342, 199
Corbelli E., Walterbos R. A. M., 2007, ApJ, 669, 315
Corbelli E., Thilker D., Zibetti S., Giovanardi C., Salucci P., 2014, A&A, 572, A23
de Blok W. J. G., Bosma A., 2002, A&A, 385, 816
de Blok W. J. G., Walter F., Brinks E., Trachternach C., Oh S. H., Kennicutt R. C. Jr, 2008, AJ, 136, 2648
Di Cintio A., Brook C. B., Macciò A. V., Stinson G. S., Knebe A., Dutton A. A., Wadsley J., 2014, MNRAS, 437, 415
Diemand J., Zemp M., Moore B., Stadel J., Carollo M., 2005, MNRAS, 364, 665
Donato F. et al., 2009, MNRAS, 397, 1169
Druard C. et al., 2014, A&A, 567, A118
Dutton A. A., Macciò A. V., 2014, MNRAS, 441, 3359
Gentile G., Salucci P., Klein U., Vergani D., Kalberla P., 2004, MNRAS, 351, 903
Gentile G., Burkert A., Salucci P., Klein U., Walter F., 2005, ApJ, 634, L145
González Delgado R. M. et al. (CALIFA Collaboration), 2014, A&A, 562, A47
Gratier P. et al., 2010, A&A, 522, A3
Hayashi E. et al., 2004, preprint (arXiv:astro-ph/0408132)
Karukes E. V., Salucci P., 2017, MNRAS, 465, 4703
Karukes E. V., Salucci P., Gentile G., 2015, A&A, 578, A13
Klypin A., Kravtsov A. V., Bullock J., Primack J., 2001, ApJ, 554, 903
Massey P., Olsen K. A. G., Hodge P. W., Strong S. B., Jacoby G. H., Schlingman W., Smith R. C., 2006, AJ, 131, 2478
Moore B., 1994, Nature, 370, 629
Navarro J. F., Frenk C. S., White S. D. M., 1996, ApJ, 462, 563
Navarro J. F., Frenk C. S., White S. D. M., 1997, ApJ, 490, 493
Oh S. H. et al., 2015, AJ, 149, 180
Palunas P., Williams T. B., 2000, AJ, 120, 2884
Persic M., Salucci P., 1988, MNRAS, 234, 131
Planck Collaboration XIII, 2016, A&A, 594, A13
Portinari L., Salucci P., 2010, A&A, 521, A82
Rubin V. C., Thonnard N., Ford W. K. Jr, 1980, ApJ, 238, 471
Salucci P., Burkert A., 2000, ApJ, 537, L9
Salucci P., Persic M., 1999, A&A, 351, 442
Salucci P., Lapi A., Tonini C., Gentile G., Yegorova I., Klein U., 2007, MNRAS, 378, 41
Salucci P., Nesti F., Gentile G., Martins C. F., 2010, A&A, 523, A83
SDSS Collaboration, 2000, AJ, 120, 1579
Zibetti S., Charlot S., Rix H. W., 2009, MNRAS, 400, 1181

This paper has been typeset from a TEX/LATEX file prepared by the author.